Doping Effects in Heavily Helium-Radiated Silicon

R. Siemieniec [(1)], H.-J. Schulze [(2)], F.-J. Niedernostheide [(2)], W. Südkamp [(3)], and J. Lutz [(4)]

[(1)] Technical University of Ilmenau / Infineon Technologies Austria AG
[(2)] Infineon Technologies AG
[(3)] Aktiv Sensor GmbH Stahnsdorf
[(4)] Technical University of Chemnitz
GERMANY

Abstract

The formation of defects modifying the effective doping concentration of He-irradiated p^+-n^--n^+ and p^+-p^--n^+ Si diodes is analyzed as a function of the annealing temperature. Capacitance-voltage and spreading-resistance measurements show that annealing at 350 °C results in the formation of an acceptor-like defect, which is tentatively attributed to the V_2O center by means of deep level transient spectroscopy measurements. Annealing at 430 °C leads to the disappearance of the acceptor-like defect. Instead, pronounced donor formation in a range close to the penetration depth of the helium ions is observed. The influence of these effects on device characteristics is discussed.

Keywords: irradiation, recombination centers, DLTS, SRP measurement, C-V measurement

INTRODUCTION

Irradiation techniques are widely used for carrier lifetime control in bipolar power devices [1-7]. Electron irradiation results in a homogenous distribution of the generated recombination centers, while proton or helium irradiation generates inhomogeneous defect profiles.
It is well-known that proton irradiation followed by annealing in a temperature range between 250°C and 500°C leads to the formation of shallow donors. For helium irradiation, the formation of acceptor-like defects can result in a compensation of the doping concentration. A well-known double acceptor is the divacancy which, however, is only stable up to annealing temperatures of about 300°C [8]. In this paper we focus on doping and compensation effects of helium irradiation after annealing at temperatures preferably ≥ 350°C.

EXPERIMENTAL DETAILS

To this end p^+-n^--n^+ (Fig. 1) and p^+-p^--n^+ (Fig. 2) test diodes were fabricated from FZ-grown silicon. The oxygen concentration in the conventionally prepared

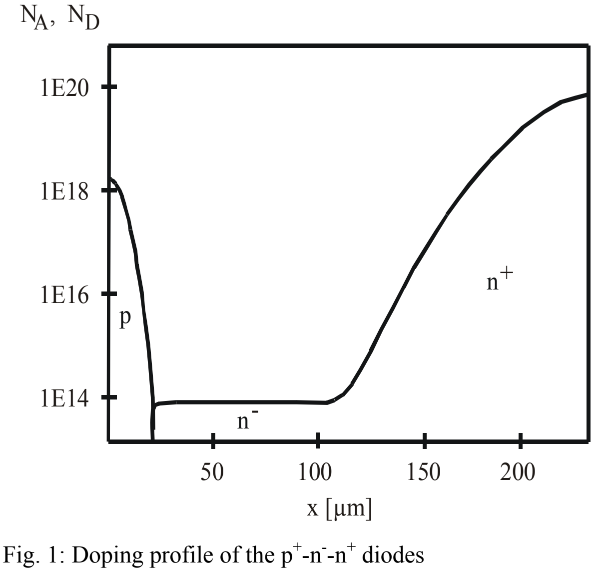

Fig. 1: Doping profile of the p^+-n^--n^+ diodes

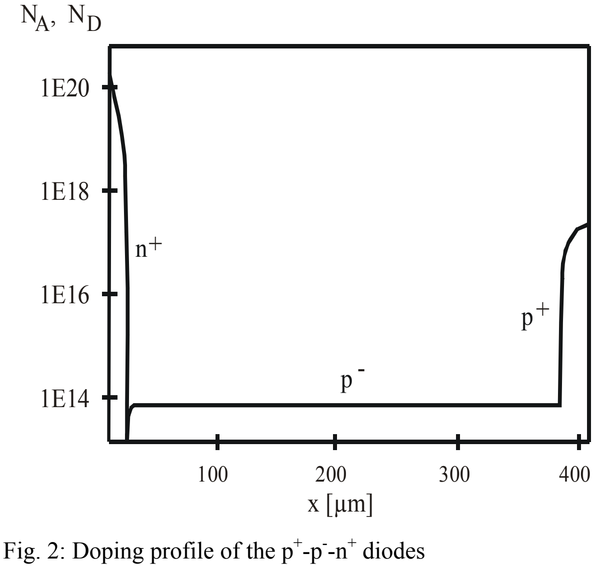

Fig. 2: Doping profile of the p^+-p^--n^+ diodes

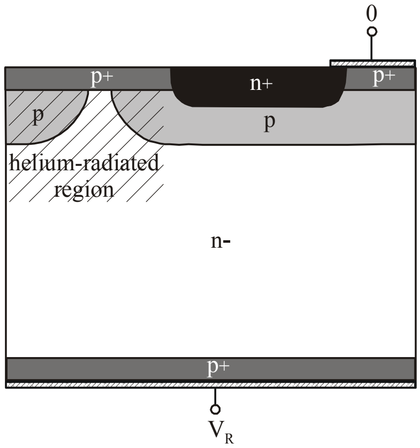

Fig. 3: Radial cross section of a test structure with a p-n$^-$ diode (left) in the center and a ring-shaped thyristor (right) connected in parallel [7]

diodes is typically higher than 10^{16}cm^{-3}. Helium irradiation was performed at room temperature with doses between 7×10^9 and 2.1×10^{12}cm^{-2}. After irradiation the samples were annealed at T = 350°C or T = 430°C in a nitrogen atmosphere for about 1h. The doping of the n-type and p-type base material is 6×10^{13}cm^{-2} and 3.3×10^{13}cm^{-2}, respectively.

Fig. 3 shows another test structure which consists of the p-n$^-$ junction and a parallel-connected thyristor [7]. The central p-region is surrounded by a p-ring which on one hand acts as a field ring and on other hand is part of the vertical n$^+$-p-n$^-$-p$^+$ structure, forming a thyristor. The p$^+$-layer, connecting the p-n$^-$ diode and the concentric p-base of the thyristor, prevents the space-charge region from reaching the surface. Together with the fact that the electric field always has maximum strength at the position of maximum curvature of the p-n$^-$ diode (when the p-layer is negatively biased with respect to the n$^-$-layer), it ensures that breakdown of the diode occurs in the bulk region. The thickness of the n$^-$-substrate is chosen sufficiently large to ensure that the maximum electric field strength at the p-n$^-$ junction meets the avalanche ionization criterion before the field reaches the anode p-layer. Thus the avalanche breakdown limits the maximum blocking voltage of the p-n$^-$ diode. The thyristor connected in parallel with the diode serves to protect the diode from damage due to breakdown. This is achieved by using the avalanche current to trigger the thyristor which turns on when a certain avalanche current is exceeded. In this case, the voltage drop across the diode is reduced to less than 10V. The typical avalanche breakdown voltage of the investigated diodes is about 5kV at room temperature.

The applied irradiation energy of 24MeV corresponds to a penetration depth of about 300µm. The irradiated area comprises not only the junction area but also a part of the concentric p-ring (Fig. 3). The local irradiation was performed by irradiating the sample through an aluminum mask with a pinhole. The irradiated samples were annealed for 4h at about 220°C. Three different He doses were applied.

Table I gives an overview of the investigated helium-irradiated samples. For defect characterization, Capacitance-Voltage (CV) measurements, Spreading-Resistance-Profiling (SRP), and Deep Level Transient Spectroscopy (DLTS) measurements were applied. The influence of the defects on the device behavior was studied by analyzing current-voltage characteristics I(V). Forward characteristics were recorded with a high-power Tektronix curve tracer model 371A by applying a linear voltage ramp during a period of 200µs. Reverse characteristics were measured with a special equipment enabling the application of single sinusoidal half-waves with a period of ≈ 80ms and voltage amplitudes up to 10kV.

COMPENSATION EFFECTS

Fig. 4 shows the doping profile in the n$^-$-base of the p$^+$-n$^-$-n$^+$ diode HeNS1 after helium irradiation for two annealing temperatures. The profiles result from CV-measurements. Minority and majority DLTS spectra of this sample are depicted in Fig. 5. The dominant peaks at E(90K) and H(195K) in the two spectra result from the VO and the COV center, respectively. The energy levels of the peaks E(230K) and E(130K) are 0.425eV

TABLE I: Sample overview

Sample	Type	Device	Helium irradiation energy	Helium irradiation dose
HeND1	n-Si	Diode	11.6 MeV	$1.4\text{x}10^{12}$ cm^{-2}
HeND2	n-Si	Diode	11.6 MeV	$2.1\text{x}10^{12}$ cm^{-2}
HeNS1	n-Si	Diode	5.4 MeV	$7\text{x}10^{10}$ cm^{-2}
HeNS2	n-Si	Diode	5.4 MeV	$7\text{x}10^{11}$ cm^{-2}
HePS	p-Si	Diode	5.4 MeV	$7\text{x}10^{9}$ cm^{-2}
HeNT1	n-Si	Diode & Thyristor	24 MeV	$3\text{x}10^{11}$ cm^{-2}
HeNT2	n-Si	Diode & Thyristor	24 MeV	$5\text{x}10^{11}$ cm^{-2}
HeNT3	n-Si	Diode & Thyristor	24 MeV	$7\text{x}10^{11}$ cm^{-2}

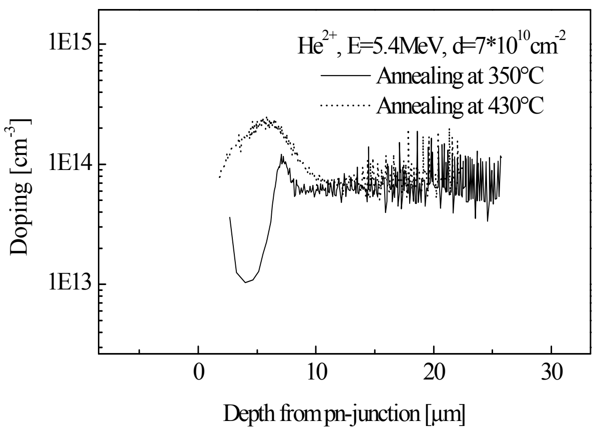

Fig. 4: Doping profile in the n^--base of the p^+-n^--n^+ diode HeNS1 after helium irradiation and annealing at two different temperatures (CV-measurement)

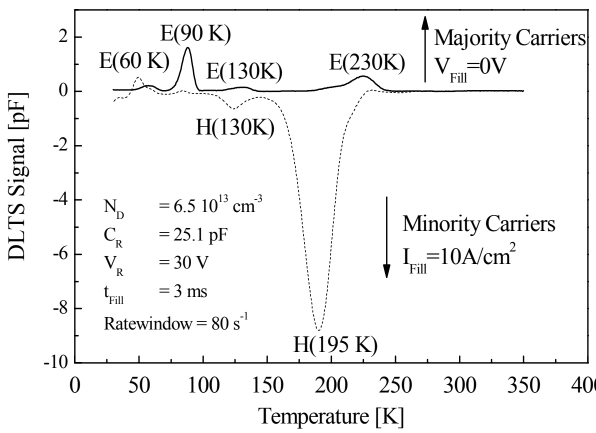

Fig. 5: Minority and majority DLTS spectrum of the p^+-n^--n^+ diode HeNS1 after helium irradiation and annealing at T=350°C

and 0.244eV below the conduction band, respectively. They are close to the energy levels of the singly negative, $V_2^{(0/-)}$, and doubly negative, $V_2^{(-/--)}$, charge states of the divacancy, which, however, should be already annealed out after annealing at 350°C. Therefore, we tentatively attribute the two peaks to the singly and doubly negative charge states of the V_2O defect, as it is suggested by the results presented in [9]. There it has been shown that a double acceptor-like defect with energy levels close to those of the divacancy is formed during divacancy annealing after proton irradiation of low-doped high-resistive oxygenated silicon.

In sample HeNS1 annealed at 350°C (Fig. 4), compensation effects are clearly visible in a depth of ≈ 5µm from the p-n^- junction, whereas the background doping in depths >10µm is unchanged. Therefore, the appearance of the center E(230K) influences the diode properties not only by modifying the charge-carrier lifetime but also due to compensation effects. In p-type silicon, E(230K) is not charged since the Fermi energy level is below the energy level of the trap. Therefore, no change in the effective doping occurs (Fig. 6, annealing at T=350°C).

DLTS measurements show that most of the centers are annealed out after a temperature treatment at 430°C (Fig. 7). In particular, the E(230K) and E(130K) signals are below the detection limit.

Fig. 8 shows the SRP measurement of the sample HeND2. In a depth of ≈ 70µm the doping is decreased, reflecting the reduction of the free carrier concentration caused by the deep centers. The depth corresponds well with the expected mean penetration depth of the implanted helium ions. Due to the compensation effect, SRP measurements are suitable for the determination of generated defect profiles, although it is difficult to draw conclusions about the defect species or exact defect concentrations.

DOPING EFFECTS BY HELIUM IRRADIATION

CV-measurements of the p^+-n^--n^+ diodes after annealing

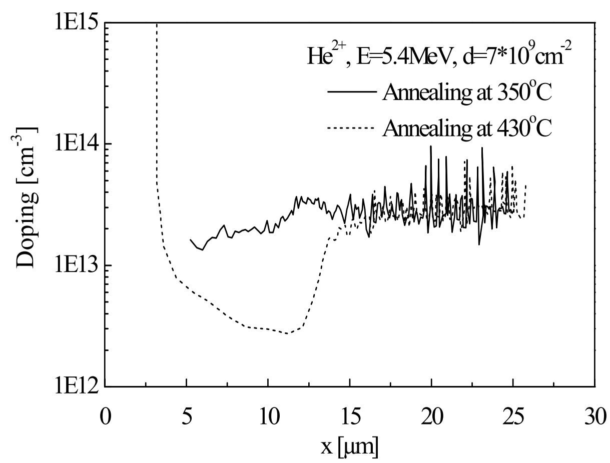

Fig. 6: Doping profile of the p^+-p^--n^+ diode HePS after helium irradiation and annealing at two different temperatures (CV-measurement)

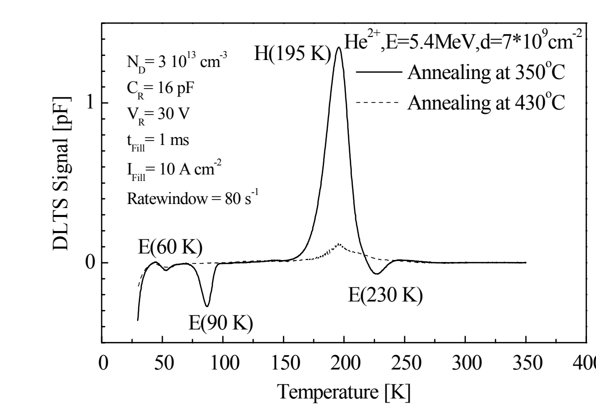

Fig. 7: Minority DLTS spectrum of p^+-p^--n^+ diode HePS after helium irradiation and annealing at two different temperatures

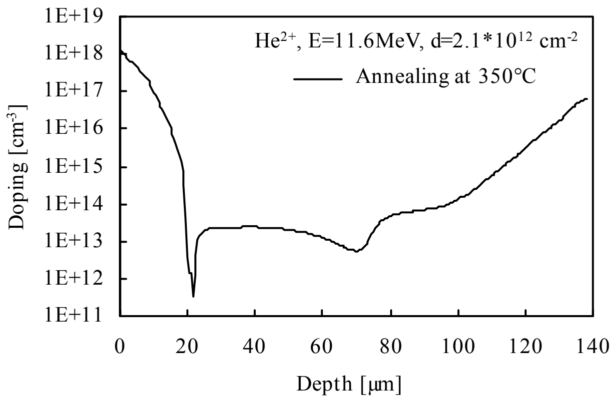

Fig. 8: Doping profile of the helium irradiated p^+-n^--n^+ diode HeND2 after annealing at T = 350°C (SRP measurement).

at a temperature of T = 430°C show a higher electron concentration in the helium irradiated area (Fig. 4), indicating the formation of donors in this area. In the p^+-p^--n^+ diodes, this donor formation results in a compensation of the p-doping. From Figs. 4 and 6, maximal donor concentrations of ≈ 2.2×10^{14} and ≈ $2.7\times10^{13}cm^{-3}$ in the helium-irradiated area can be estimated for helium doses of 7×10^{10} and $7\times10^{9}cm^{-2}$ after annealing at 430°C.

Since signals of donor-like defects are not observable in the DLTS spectra (Fig. 7), we attribute the formation of these donors in the helium-irradiated area to the formation of Thermal Double Donors (TDDs). TDD formation is well-known from Cz-grown silicon with a high oxygen concentration after annealing at temperatures preferably between 350°C and 500°C. They consist of a core, [110] chains of <001> Si interstitials, surrounded by different shells containing oxygen. Further details can be found in Ref. [10].

In our samples the oxygen concentration is relatively high due to the preparation conditions of the diodes, which include long thermal diffusion steps (e.g., to create the deep n^+-layer in the p^+-n^--n^+ diodes, cf. Fig. 1). This assumption is also consistent with the existence of E(60K) in both DLTS spectra (Figs. 5 and 7), since it has been shown, that E(60K) arises from a oxygen-related complex which is found only after long thermal treatment [11].

Similar TDD formation has been observed also in electron–irradiated GTO thyristors fabricated from n-type FZ-grown Silicon. The breakdown voltage of these GTO thyristors is limited by the punch-through effect and reaches a maximum value after annealing at T ≈ 450°C. From this result it can be concluded that the thermal donor concentration in the n-base of the GTO thyristor has a maximum at this annealing temperature, which is consistent with the well-known TDD formation behavior in Cz-grown silicon.

It is worth to mention that DLTS measurements are affected by the effective background doping due to two effects: First, the maximum detectable defect concentration depends on the background. Second, the spatial resolution of defect profiles determined by making use of the fill-pulse technique [12] is improved for higher doping concentrations. A measure for the spatial resolution [13] is given by the Debye length L_D

$$L_D = \sqrt{\frac{2\,\varepsilon_r \varepsilon_0\, V_T}{q\, N_D}}\ ,$$

where ε_r and ε_0 are the relative and absolute permittivity, V_T denotes the thermal voltage, q the electric charge and N_D the background concentration. Thus, under certain conditions, the effect of an increased doping due to helium irradiation can be exploited to improve the spatial resolution of defect profiles.

INFLUENCE ON DEVICE CHARACTERISTICS

Influence on forward characteristics

The generated number of acceptor-states E(230K) in the diode HeND2 is sufficiently large to cause a clear compensation of the background doping (Fig. 8). This compensation also influences the forward current-voltage I(V) characteristics of this device.

In Fig. 9, the forward characteristics of sample HeND2 are shown for different operating temperatures. The measurements were performed using a Tektronix curve tracer model 371A applying voltage ramps with a length of about 200µs. Due to the generated recombination centers not only the forward voltage drop across the device is increased, but the usually unique I(V) characteristic may even change to a characteristic with Negative Differential Resistance (NDR) for low operating temperatures. Such an effect - though only weakly distinctive - is reflected in the I(V) characteristic at an operating temperature T = 250K.

As possible reasons for this effect, two mechanisms can be considered for the appearance of the NDR region. First, similar S-shaped I(V)-characteristics are well-known from Au-doped silicon pin-diodes [14], where c_p

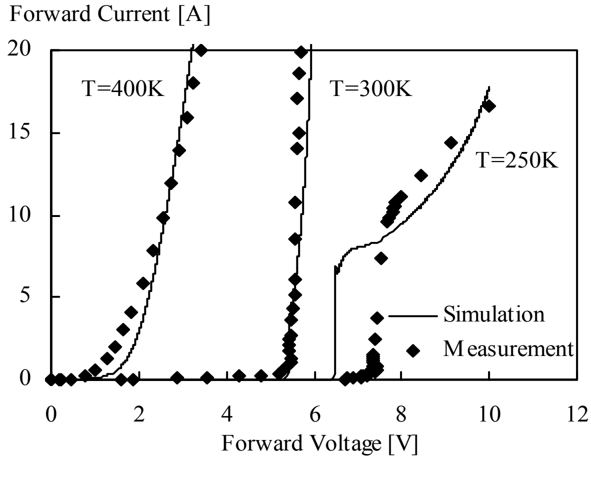

Fig. 9: Forward characteristics of sample HeHD2

> c_n of the acceptor-like near midgap level together with the injection dependent trap occupation causes the bistability. Second, the strong helium irradiation causes so much acceptor-like defects that a certain area of the n^--base close top the penetration depth of the helium ions is overcompensated and transforms into a p-type region. Therefore, the diode structure changes into a thyristor-like structure for which an S-shaped I(V) characteristic with a NDR-region is well-known. In this case, the observed temperature-dependence of the I(V) characteristics in Fig. 9 is due to the dependence of the transistor gain.
As it is further shown in Fig. 9, device simulation is able to predict this behavior. In these simulations, the voltage was linearly ramped, similar to the measurement. Three centers, E(90K), E(230K) and H(195K), are used for device simulations. For E(90K) and H(195K), the parameters according to previous work are used [13]. In case of E(230K), the hole capture rate of this trap is modified towards a larger effective emission rate as suggested in [15]. The bistable I(V)-characteristic is essentially due to the fact that the ratio of the hole and the electron capture cross section of the E(230K) defect level, c_p/c_n, increases with decreasing operating temperature.

Influence on blocking voltage

Effects induced by helium irradiation can be exploited for the adjustment of the blocking voltage of p-n^- junctions. Fig. 10 shows the increase in the breakdown voltage after helium irradiation and annealing as a function of the irradiation dose for the diode test structures HeNT1-3. The breakdown voltage of the diodes increases monotonically with the irradiation dose by several hundred volts. Annealing of these samples was performed at T = 220°C. Therefore, the acceptor-like divacancy still exists and may contribute to compensation effects.

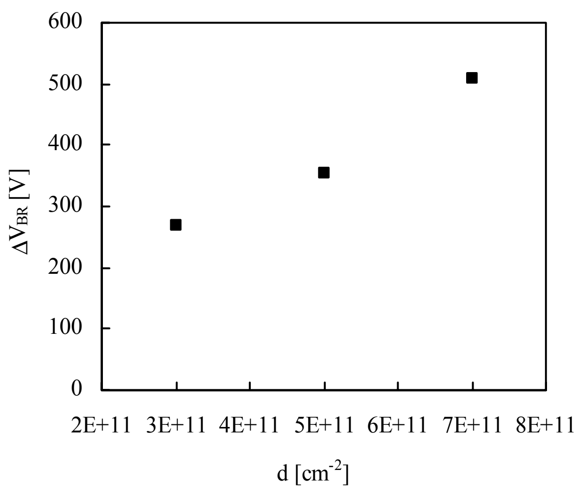

Fig. 10: Increase of forward breakdown voltage of 5 kV p-n-diode test structures HeNT1-3 after 24 MeV helium irradiation at T = 300 K [7]. Plotted values are mean values from measurements on several samples implanted with the same dose

According to [16] the formation of divacancy clusters is possible after irradiation with particles at high doses. Due to the high divacancy concentration (≈ 10^{20} cm^{-3}) inside the clusters, interaction of the energy levels between physically different divacancy levels is possible. Due to this interaction the stationary negatively-charged divacancy concentration inside the SCR can increase up to three orders of magnitude. Thus, such cluster formation could explain the relatively large voltage increase. However, further investigations are necessary to confirm this assumption.
The low temperature budget during annealing is advantageous, since it enables an adjustment of the breakdown voltage even after the fabrication of a device is completed. It should be mentioned that the reverse leakage current of a p-n junction grows with increasing doses. However, when small diodes are used, e.g. as breakover diodes to protect areas of larger size [7], this drawback is of minor importance.

CONCLUSION

In this work, the influence of helium irradiation on the background doping has been investigated. Compensation effects were studied by CV, SRP and DLTS measurements using test diodes based on n-type as well as p-type substrate material. Depending on the annealing conditions, divacancies and the V_2O-defects are assumed to be responsible for the observed compensation effects at annealing temperatures ≤ 350°C.
At annealing temperatures of 430°C we observe an increase in the donor concentration in the area close to the maximum penetration depth of the helium ions. This is most probably caused by the formation of TDDs.
It has been shown that He-irradiation can be used to adjust the breakdown voltage of a p-n junction. This effect is most probably related to the formation of divacancy clusters, where interaction of the different divacancy levels becomes probable due to the large defect densities within the cluster. Consequently the total concentration of charged divacancies becomes some orders of magnitude larger than expected by the common assumption of non-clustered divacancy complexes.

ACKNOWLEDGEMENTS

The authors thank Ms. Pellkofer (SEMIKRON Elektronik GmbH Nürnberg, Germany) for the preparation of the p^+-n^--n^+ and the p^+-p^--n^+ diodes and Dr. Möller (Institute Fresenius Dresden, Germany) for performing the SRP measurements and for helpful discussions.

REFERENCES

[1]. Robb, F., Wau, I., and Ju, S.: Increasing the Switching Speed of High-Voltage IGBTs, Proc. ISPSD, 251-254, Weimar, 1997

[2]. Nakagawa, T., Satoh, K., Yamamoto, M., Hirasawa, K. and Ohta, K.: 8kV/3.6kA Light Triggered Thyristor, Proc. ISPSD, 175-180, Yokohama, 1995

[3]. Lutz, J.: Axial Recombination Centre Technology for Freewheeling Diodes, Proc. EPE, 1502-1506, Trondheim, 1997

[4]. Siemieniec, R. and Lutz, J.: Possibilities and limits of axial lifetime control by radiation induced centres in fast recovery diodes, Microelectronics Journal, 35 (3), 259-267, 2004

[5]. Kaminski, N., Galster, N., Linder, S., Ng, C. and Francis, R.: 1200V Merged PIN Schottky Diode with Soft Recovery and Positive Temperature Coefficient, Proc. EPE, Lausanne, 1999

[6]. Vobecký, J., Hazdra, P. and Homola, J.: Optimization of power diode characteristics by means of ion irradiation, IEEE Transactions on Electron Devices, 43, 2283-2289, 1996

[7]. Niedernostheide, F.-J., Schmitt, M., Schulze, H.-J., Kellner-Werdehausen, U., Frohnmeyer, A. and Wachutka, G.: Analysis of Radiation-Induced Defects and Performance Conditioning in High-Power Devices, Journal of the Electrochemical Society, 150 (1), G15-G21, 2003

[8]. Watkins, G.D.: Vacancies and Interstitials and their interaction with impurities in c-Si, Properties of Crystalline Silicon, ed. By R. Hull, *EMIS Datareviews Series*, No. 20, Inspec, 643-652, London, 1999

[9]. Monakhov, E.V, Avset, B.S., Hallen, A., and Svensson, B.G.: Formation of a double acceptor centre during divacancy annealing in low-doped high-purity oxygenated Si, Phys. Rev. B, 65, 233207, 2002

[10]. C.A.J. Ammerlaan: Thermal double donors in c-Si, Properties of Crystalline Silicon, ed. By R. Hull, *EMIS Datareviews Series*, No. 20, Inspec, 663-668, London, 1999

[11]. Brotherton, S.D. and Bradley, P.: Defect production and lifetime control in electron and gamma-irradiated Silicon, Journal of Applied Physics, 53 (8):5720-5732, 1982

[12]. Südkamp, W. and Gerlach, W.: Untersuchung tiefer Zentren und Bauelementesimulation, VDI/VDE-IT - Reihe Innovationen in der Mikrosystemtechnik, 1999

[13]. Siemieniec, R.: Simulation von Leistungs-bauelementen mit durch Bestrahlungsverfahren eingestellter Trägerlebensdauer, Ph.D. thesis TU Ilmenau, BoD Verlag Norderstedt, 2003

[14]. Dudeck, I. and Kassing, R.: The influence of recombination data on the I-V characteristics of silicon p-i-n diodes, J. Appl. Phys. 48 (11), 4786-4790, 1977

[15]. Hazdra, P., Rubeš, J. and Vobecký, J.: Divacancy profiles in MeV helium irradiated silicon from reverse I-V measurement, Nuclear Instruments and Methods in Physics Research, B 159, 207-217, 1999

[16]. Gill, K., Hall, G. and MacEvoy, B.: Bulk damage effects in irradiated silicon detectors due to clustered divacancies, Journal of Applied Physics, 82, 126-136, 1997

Addresses of the authors

Ralf Siemieniec, Infineon Technologies Austria AG, Siemensstraße 2, A-9500 Villach, Austria, e-mail: ralf.siemieniec@infineon.com

Hans-Joachim Schulze, Infineon Technologies AG, Automotive and Industrial, Balanstraße 59, D-81541 Munich, Germany, e-mail: hans-joachim.schulze@infineon.com

Franz-Josef Niedernostheide, Infineon Technologies AG, Automotive and Industrial, Balanstraße 59, D-81541 Munich, Germany, e-mail: franz-josef.niedernostheide@infineon.com

Winfried Südkamp, Aktiv Sensor GmbH, Ruhlsdorfer Str. 95, Gebäude 4, D-14532 Stahnsdorf, Germany, e-mail: wsuedkamp@aktiv-sensor.de

Josef Lutz, Technical University of Chemnitz, Faculty of Electrical Engineering and Information Technology, D-09107 Chemnitz, Germany, e-mail: josef.lutz@infotech.tu-chemnitz.de